

Modelling failure of joining zones during forming of hybrid parts

WESTER Hendrik^{1,a,*}, STOCKBURGER Eugen^{1,b}, PEDDINGHAUS Simon^{1,c},
UHE Johanna^{1,d} and BEHRENS Bernd-Arno^{1,e}

¹Institute of Forming Technology and Machines (IFUM), Leibniz Universität Hannover,
An der Universität 2, 30823 Garbsen, Germany

^awester@ifum.uni-hannover.de, ^bstockburger@ifum.uni-hannover.de,

^cpeddinghaus@ifum.uni-hannover.de, ^duhe@ifum.uni-hannover.de,

^ebehrens@ifum.uni-hannover.de

Keywords: Pre-Joined Hybrid Semi-Finished Parts, Numerical Modelling, Cohesive Zones, Local Tensile Tests

Abstract. Combining diverse materials enables the use of the positive properties of the individual material in one component. Hybrid material combinations therefore offer great potential for meeting the increasing demand on highly loaded components. The use of hybrid pre-joined semi-finished products simplifies joining processes through the use of simple geometries. However, the use of pre-joined hybrid semi-finished products also results in new challenges for the following process chain. For example, the materials steel and aluminium may form brittle intermetallic phases in the joining zone, which can be damaged in the following forming process under the effect of thermo-mechanical loads and thus lead to a weak point in the final part. Due to their small thickness as well as their position in the component, the analysis of the joining zone is only possible by complex destructive testing methods. FE simulation therefore offers an efficient way to analyse the development of damage in the process design and to reduce damage by process modifications. Therefore, within this study a damage model based on cohesive zone elements is implemented in the FE software MSC Marc 2018 and calibrated using experimental local tensile tests performed under process relevant conditions.

Introduction

Given the constant shortage of energy as well as raw material resources and the associated costs, the conservation of resources in all areas is of great importance to society as a whole. The manufacturing industry in particular offers a wide range of potentials that extend across development, production and subsequent part usage. The resulting steadily increasing demands on components in terms of strength, functional integration and weight can no longer be met by monolithic materials. In this context, hybrid components show great potential, due to the possibility to locally use suitable materials at the right place. In recent years, composite forging has developed considerably for the production of hybrid components such as gear elements [1], whereby the semi-finished products are joined during the forging process. For example, hybrid bulk metal components such as connecting rods, wheel hubs and control arms are manufactured by Leiber Group GmbH & Co. KG, where the material composite is produced in particular by frictional and interlocking connection [2].

Groche et al. studied the influence of process variables on the welding of steel and aluminium by cold extrusion [3]. The billets' initial microstructural states, height ratio as well as the treatment of welding surfaces were investigated. They found that the precipitation hardened state of aluminium alloys are more suited for processing than the soft annealed state if the intention is to obtain a sound bonding behaviour with steel. An innovative manufacturing route for the production of hybrid components named Tailored Forming was developed using hybrid pre-joined semi-finished [4]. The material combination of steel and aluminium has great potential for industrial



application in hybrid components. On the one hand, the high lightweight potential of aluminium alloys can be exploited. On the other hand, components that are subject to special requirements in terms of strength and load-bearing capacity can be made of steel. However, use of hybrid components also result in new challenges with regard to component design and the development as well as implementation of manufacturing processes. When using dissimilar metallic material combinations, the bonding zone in particular represents a critical point during forming and in the final component. Therefore, it requires special consideration. Previous investigations show that during impact extrusion critical tensile stresses occur within the joining zone which can lead to local rupture [5]. However, the joining zone within the process as well as in the final component can only be analysed at great expense and in destructive tests. Therefore, this work focuses on the experimental analysis of bonding strength of hybrid pre-joined semi-finished parts consisting of steel and aluminium taking into account process relevant temperatures. Based on the results a newly developed material model [6] for describing the damage development within the joining zone is calibrated and implemented in the commercial FE software MSC Marc.

Materials and Methods

Tailored Forming process chain.

The processing of pre-joined hybrid semi-finished products requires adapted process chains. In particular, the diverging material properties and the resulting requirements on the forming process must be taken into account for material combinations of different types, such as steel and aluminium. The Tailored Forming process chain for manufacturing a hybrid demonstrator shaft in the material combination 1.3505 (100Cr6) and 3.2315 (EN AW-6082) is shown schematically in Fig. 1 and described in detail in the following. The joining of the steel and aluminium is carried out by friction welding. Afterwards, the part is heated inductively. Previous studies have shown that temperature control is of particular importance for the forming of hybrid steel-aluminium semi-finished products. Therefore, an inhomogeneous temperature field is set via induction heating [7]. The aim is to heat the steel as much as possible and keep the aluminium as cold as possible, to match the flow stresses of both materials. After heating, forming is carried out by an impact extrusion process on a screw press (Lasco SPR 500). The process takes 0.12 s, whereby the diameter is reduced by 31.5 %. Finally, the part is finished by turning and a high-performance component is created.

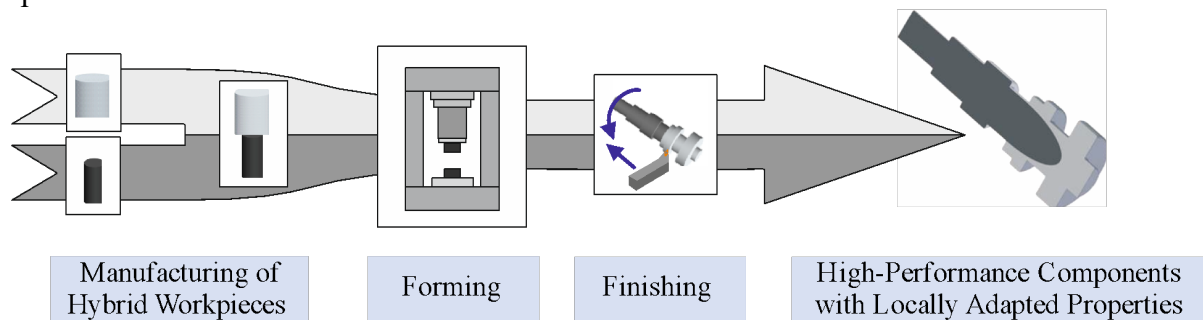


Fig. 1. Tailored Forming process chain for the production of hybrid shafts according to [8].

Thermo-mechanical material modelling.

In order to describe the material behaviour of the used aluminium EN AW-6082, flow curves are taken from previous work [5]. For the 100Cr6, flow curves from Simufact Forming 16.0 database are used to model the steel. A comparison of the used flow curves for different temperatures and a strain rate of 1 s^{-1} is given in Fig. 2. The comparison of the yield stresses of the materials clearly shows that inhomogeneous heating is required to adjust the yield stress levels. Comparable flow stress levels can be defined between 600°C and 1000°C in the case of 100Cr6 and between 20°C and 300°C in the case of the EN AW-6082. The temperature and strain rate

dependent flow curves were implemented in the FE software Simufact Forming 16 and MSC MARC Mentat 2018 for a simulation of the inductive heating and the impact extrusion.

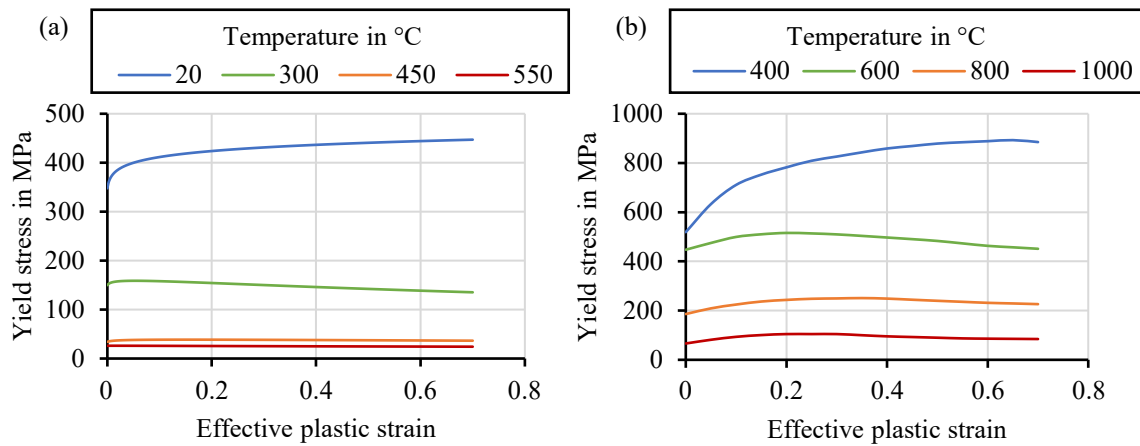


Fig. 2. Flow curves for various temperatures and a strain rate of 1 s^{-1} for EN AW-6082 (a) and 100Cr6 (b).

Analysis of local bonding strength.

The resulting local bonding strength after friction welding is investigated by local tensile tests (as shown in Fig. 3) using miniaturised sample geometries on the forming dilatometer DIL805A/D+T. The use of miniaturised samples with a thickness of 1 mm allows local analysis of bond strength as a function of the semi-finished product diameter. In order to physically map the critical thermo-mechanical stresses of the hybrid semi-finished products, which lead to failure of the joining zone, the tensile tests are carried out at various testing temperatures. The temperatures for tensile testing are determined based on numerically calculated temperatures in the joining zone during impact extrusion. The tensile tests are performed at a quasi-static strain rate of 0.001 s^{-1} .

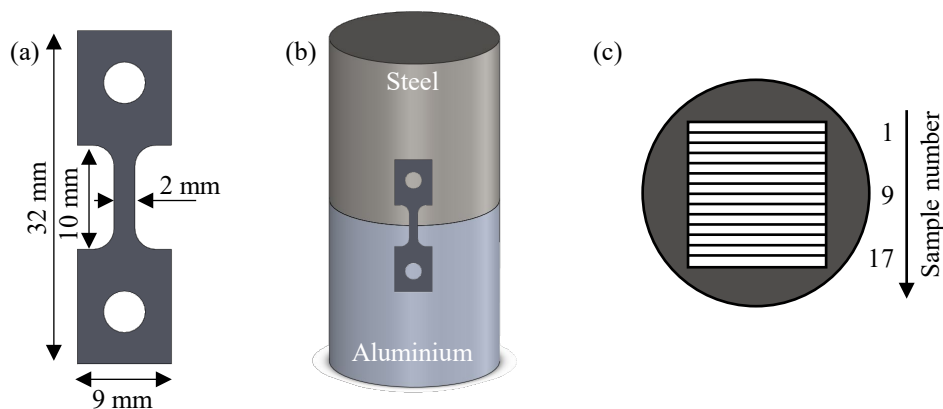


Fig. 3. Procedure for characterising the local bonding strength of joining zones: sample geometry (a) and sectional view (b) as well as top view (c) of the sample extraction area.

Numerical model of induction heating and impact extrusion.

Numerical simulation allows a realistic determination of temperature distribution during the impact extrusion process. To determine process relevant testing temperature for the tensile tests a numerical model representing induction heating as well as the forming process was first developed using the commercial FE software Simufact Forming 16. The model for induction heating consists of the hybrid billet placed within the induction coil. During heating, only the steel is heated

inductively, the aluminium is heated by thermal conduction. Between steel and aluminium an adhesive contact was defined and an intermetallic layer of $0.07 \mu\text{m}$ was assumed [9] with a thermal conductivity of 10 W/mK according to Nacke [10]. Boundary conditions like current, time and frequency were taken from experiments and set as input. Thermal material data was defined based on Simufact Forming 16 database. The relative permeability was determined by Behrens et al. using the method described in [7]. The calculated inhomogeneous temperature field after induction heating is transferred to the semi-finished product of the impact extrusion model. The elastic-plastic material behaviour of steel and aluminium parts is modelled as shown before. The impact extrusion tool system consists of a die and a punch, which are modelled as rigid heat conducting bodies with an initial temperature of $250 \text{ }^\circ\text{C}$. Friction is modelled by the combined friction model consisting of the Tresca formulation with $m = 0.3$ and the Coulomb formulation with $\mu = 0.1$. The press kinematics were derived from experimental data of the used screw press and considered within the numerical model. However, the modelling of the joining zone requires cohesive zone elements. Since these are not available in Simufact Forming, another model of the extrusion process was created in the FE software MSC Marc 2018.

Damage modelling.

The brittle material behaviour of the joining zone is of particular importance in the forming of hybrid semi-finished products. However, the very low thickness of the intermetallic phase compared to the dimensions of the semi-finished products is challenging. Conventionally, the damage in thin layers is modelled by flat cohesive zone elements [11]. Their constitutive behaviour is described via traction separation laws, which take into account expansion under normal or shear loading. However, cohesive zone elements are flat and therefore cannot be used to describe the constitutive behaviour in bulk metal forming. In this context, Töller et al. developed a new concept for damage modelling of thin joining zones [6]. As shown in Fig. 4, the model combines the damage to cohesive zone elements described by traction separation behaviour with damage induced by severe membrane deformation such as stretching, which can occur during forming of hybrid semi-finished parts within the joining zone. Membrane deformation is considered using the Internal Thickness Extrapolation (InTex) concept. This enables the use of cohesive zone elements for bulk forming simulation by consideration of a thickness within the element formulation. Traction within the cohesive elements are calculated from resulting separations δ and stiffness k with a linear relationship. As proposed by Töller, a large but finite artificial stiffness k is introduced. The stiffness can be interpreted as a penalty parameter to model the brittle behaviour of thin intermetallic phases. Due to the use of effective tractions the tractions are reduced by local prevailing damage D . Thus, a local pre-damage as well as the damage by membrane deformation during forming process can be taken into account. A detailed description of the developed model can be found in [6]. To model the damage in joining zones of semi-finished hybrid parts during forming processes within the Tailored Forming process chain, the modelling concept was implemented in the cohesive element formulation of the commercial FE software MSC Marc 2018 using the user subroutine UCOHESIVE. This software was selected because, contrary to Simufact Forming, it supports the use of cohesive zone elements. The presented work deals with the development of a methodology determining the model parameters taking into account the thermo-mechanical process boundary conditions. The calibration of the model was done inversely by numerical simulation of the local tensile tests. The elastic-plastic material behaviour of steel and aluminium was described as shown before. The displacements are applied via the nodes on the end sample faces according to experimental tensile test. The isothermal test temperatures are imposed on all nodes of the model via a thermal boundary condition. The joining zone in the centre of the sample is modelled via cohesive zone elements. The failure time determined from the experimental force-displacement curves and the applied force are used as the target variables. Since the focus is on determining the value $t_{i,\text{max}}$ and only samples with a joining zone normal to the direction of

loading are analysed, the value for $t_{s,max}$ is specified analogously to the procedure in [6] via the ratio $t_{t,max}/t_{s,max} = 1.22$. Damage due to membrane deformation is described via the Lemaitre damage model [12]. The parameters $s = 1$ and $S = 0.34$ for the description of the Lemaitre damage model are chosen accordingly to [6].

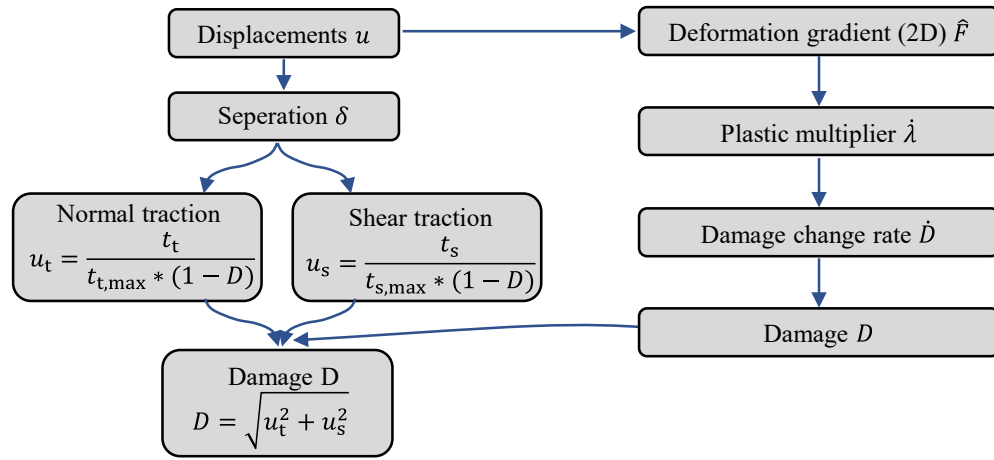


Fig. 4. Schematic representation of damage model for thin intermetallic phase.

Results

Numerical analysis of induction heating and impact extrusion.

As shown in Fig. 2, the flow curves of the materials differ significantly demonstrating the need for inhomogeneous heating to adjust the material flow properties for impact extrusion. According to the flow curves, the steel semi-finished product should be heated to 900°C and the aluminium semi-finished product to 300°C for homogenous material flow properties. The adjustability of the temperature field was investigated by experimental and numerical analyses of the inductive heating. The numerical simulation is used for the process analysis regarding the temperature development in order to define proper testing temperatures, as shown in Fig. 5 (a). Analogously to the experimental process, the semi-finished steel product is inductively heated for 25 s. A maximum temperature of 900°C is reached. During the transfer period of 5 s until the start of the impact extrusion, the maximum temperature drops to approx. 800°C due to heat transfer processes. The aluminium is heated only by heat conduction from the steel and reaches a maximum temperature of approx. 400°C after 30 s before forming. The maximum temperature of the joining zone is 420°C before the forming process starts. Due to the short forming process period of only 0.12 s, no significant temperature change is observed during forming, as shown in Fig. 5 (b). Fig. 5 (c) and (d) display the temperature distribution of the inhomogeneous heated semi-finished product after the transfer period from the induction heating and before the impact extrusion, both at the process time of 30 s. Based on this analysis, the bond strength of the joining zone is investigated in local tensile tests at the process relevant temperatures of 400°C and 450°C. The results of the tensile tests are used to determine the bond strength of the joint zone.

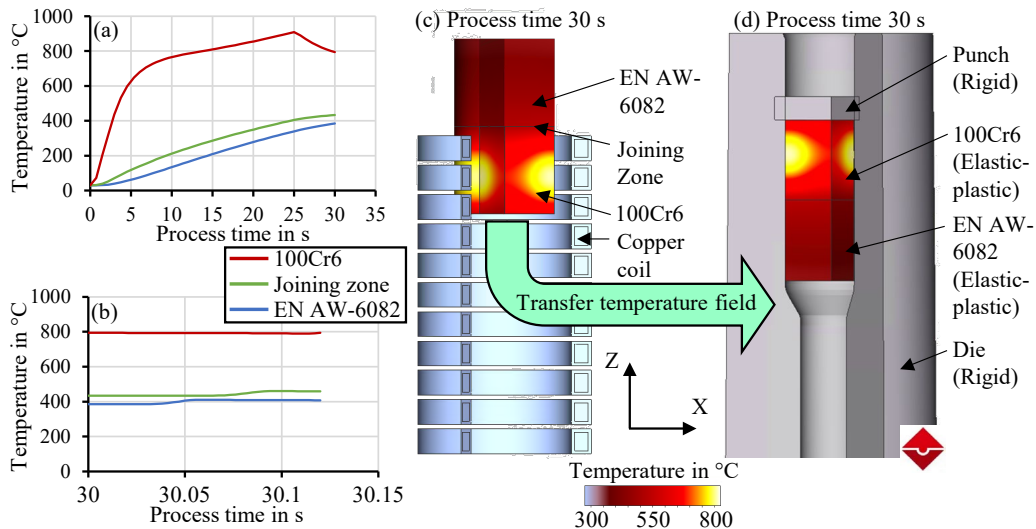


Fig. 5. Temperature development during induction heating (a) and impact extrusion (b) as well as coupled numerical process chain consisting of induction heating process (c) and impact extrusion (d).

Local bond strength and damage model calibration.

Fig. 6 shows the determined bond strengths as a function of temperature and the sample extraction area from the semi-finished product for a load normal to the joining zone. The sample extraction area can be found in Fig. 3 (c). Therefore, the bond strengths of samples with low and high numbers correspond to the edge area and the sample no. 9 to no. 11 to the bond strength in the centre of the friction-welded semi-finished product. For sample no. 10 no results could be determined at room temperature, because the samples failed directly.

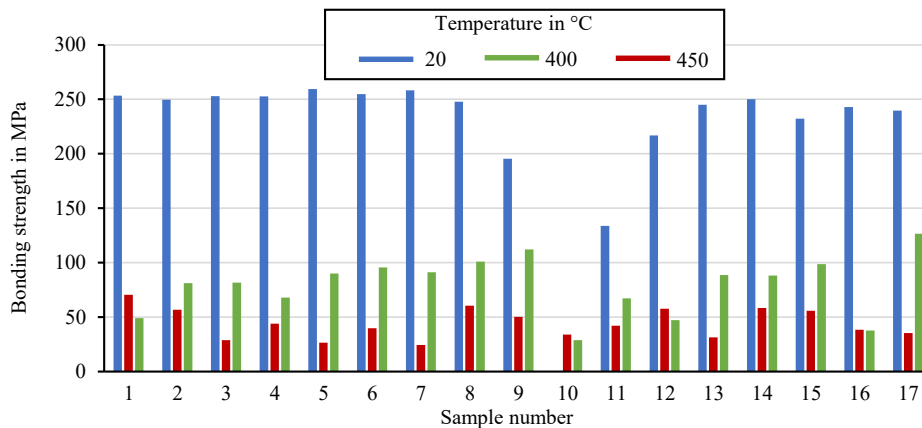


Fig. 6. Bond strength for normal loading depending on temperature and sample extraction area.

In particular, the tests at room temperature show a strong dependence on the removal position. Thus, the samples from the edge region exhibit a significantly higher bond strength than samples from the middle region. The tests also show a clear dependence on temperature. With increasing temperature, the bond strength decreases significantly. An optical analysis of the fracture surfaces showed a failure in the joining zone for all samples. Thus, at the process relevant temperatures compared to room temperature, even low tensile loads are critical with regard to a possible local failure of the joining zone and must be particularly taken into account in the process design.

As the stress-strain curve in Fig 7 (a) shows exemplarily for the sample 4 at 20°C, the samples from the edge region exhibit significant plastic deformation. An optical analysis of the samples shows a clear necking in the aluminium region and a failure of the monolithic material aluminium. Thus, the bond strength is greater than the tensile strength of the aluminium. Samples from the middle region like sample 9 in Fig 7 (b) show lower bond strengths and no pronounced plastic deformation. An optical analysis of the fracture zone shows failure in the joining zone without significant plastic deformation of the monolithic materials. The bond strength is thus below that of the weaker monolithic material aluminium and can be determined directly. The strong dependence of the bond strength is due to the process characteristics of friction welding. While high relative velocities prevail in the edge zone, which cause the oxide layer on the aluminium to break up and flow out, the relative velocity decreases toward the centre of the semi-finished product [13].

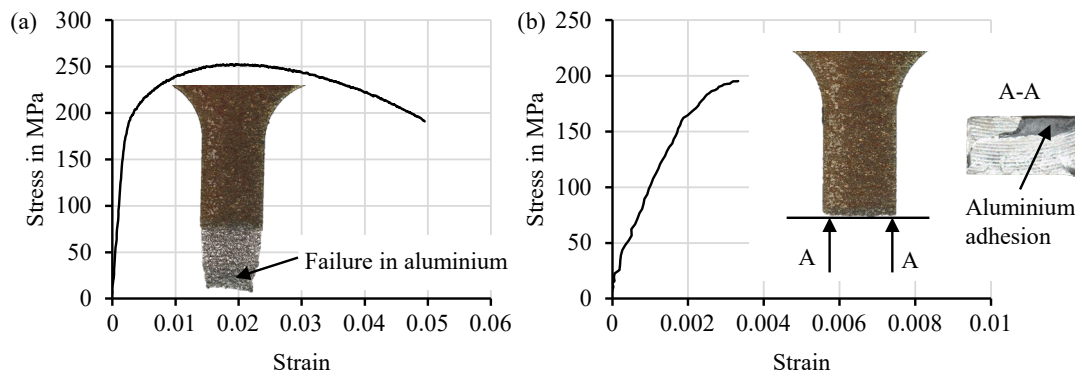


Fig. 7. Stress-strain curves and optical images after failure for sample 4 (a) and sample 9 (b) at 20°C.

For the determination of $t_{t,max}$ to calibrate the damage model, the performed tensile tests were mapped in the FE software MSC Marc 2018 with the corresponding experimental boundary conditions. A representation of the numerical model of the tensile test is given in Fig. 8. The temperature dependent values of $t_{t,max}$ were determined numerically iteratively by comparison with the experimental force-displacement curves and the time of failure. For the calibration, the sample no. 8 is used. This specimen exhibited the highest bond strength at failure in the joining zone without significant plastic deformation of the aluminium part. Thus, the calculated stress can be directly related to the bonding strength.

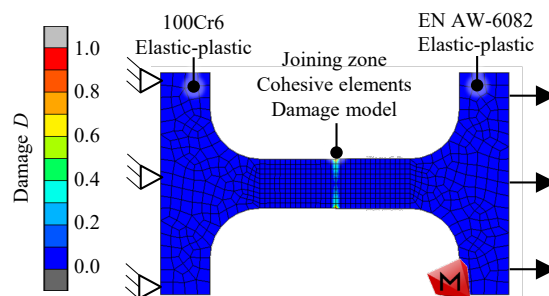


Fig. 8. Numerical model of tension test with joining zone modelled by means of cohesive elements.

A comparison of the force-displacement curves for the temperatures considered using the corresponding value for the damage parameter $t_{t,max}$ can be found in Fig. 9 (a) to (c). The

numerically inverse determined values can be found in Fig. 9 (d). The force-displacement curves agree well, so that the model and also the methodology can be considered validated. The force level at fracture is well predicted. However, there are small deviations regarding the length change at fracture between experiment and simulation. This is probably due to a slight plastic deformation of the specimens in the aluminium part, which is underestimated in the simulation. For a later application of the numerical representation of the impact extrusion process considering the damage of the joining zone, the local distribution of the maximal bond strength according to the findings of the local tensile tests has to be taken into account by defining local initial values for the pre-damage D and maximal bond strength $t_{t,max}$. For samples extracted at larger diameters of the semi-finished product, which show plastic deformation and failure of the aluminium, the achievable bond strength $t_{t,max}$ is increased by 25 % for later application. The decrease of the bonding strength with decreasing diameter towards the centre of the semi-finished product can be taken into account in the application by the damage parameter D as pre-damage, which is scaled according to the results in Fig. 6 taking into account the local position.

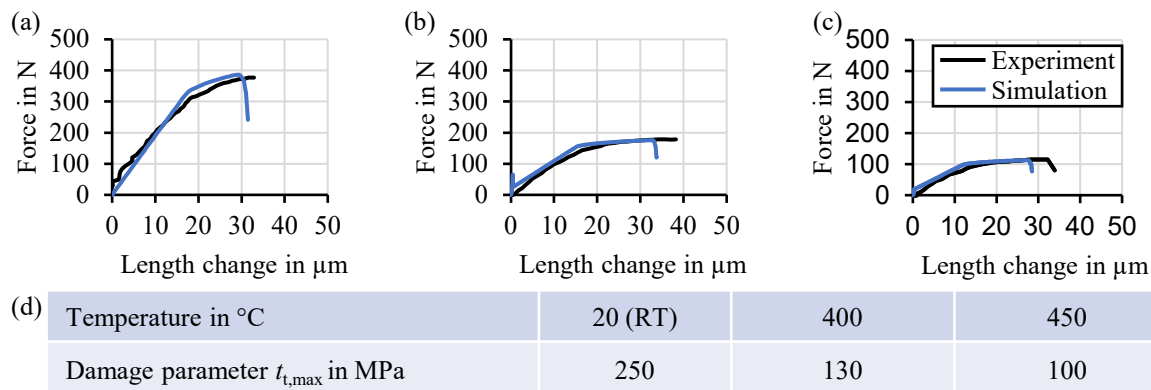


Fig. 9. Force-displacement curves from experiment and simulation at a temperature of 20°C (a), 400°C (b) and 450°C (c) for sample no. 8 as well as the determined temperature dependent damage parameter $t_{t,max}$ (d).

For a numerical analysis of the impact extrusion taking the joining zone into account, the process was also modelled in MSC Marc 2018. The boundary conditions were selected analogously to the described procedure for the tensile test simulations. As in the tensile tests, the joining zone itself is represented by cohesive zone elements. Since the damage model requires a three-dimensional mapping, a quarter model is used. The inhomogeneous temperature distribution is taken from the inductive heating in analogy to the procedure in Simufact Forming and imposed as initial temperature on the nodes in the Marc model. The extrapolation of temperature results from the nodes within the 2D space of the induction heating simulation (Simufact Forming) to the 3D space of the impact extrusion process model (MARC) is done via the radial relation $r = \sqrt{x^2 + x^2}$. The von Mises stress distribution after forming is shown in Fig. 10 (a). Due to heating, very low stresses are present, especially in the aluminium. In the steel part, higher stresses are present at the transition area to the aluminium. This is due to the physically induced inhomogeneous temperature distribution also in the steel component. As can be seen in Fig. 5, lower temperatures occur in the transition area of the steel due to heat conduction effects into the aluminium. This cannot be completely prevented even by adapted induction heating. Fig. 10 (b) shows the distribution of damage before and after forming. As can be seen, initial damage to the joining zone is already present before forming for small diameters in order to map the influence of the friction welding process on the local bond strength. After forming, damage can be seen in the

central area of the joining zone. This damage has already been observed by Behrens et al. for impact extrusion of the steel/aluminium combination 20MnCr5/EN AW-6082 pre-joined by laser welding, as shown in Fig. 10 (c) [14]. For this material combination, it was experimentally proven that an applied counterpressure prevents tearing of the joining zone by reducing the tensile stresses present. In subsequent investigations, other parameters of the damage model must therefore be further identified using the methodology described here and finally validated on the basis of experimental impact extrusion tests.

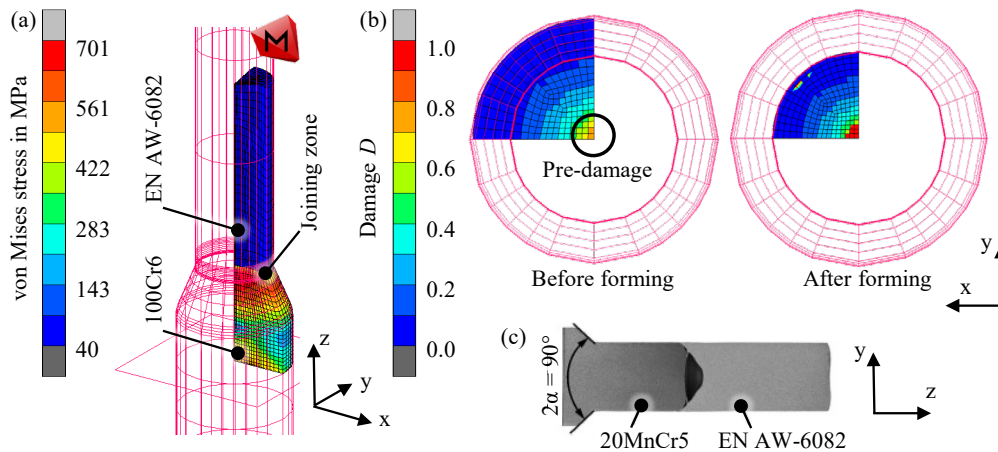


Fig. 10. von Mises stress after impact extrusion (a), damage within the joining zone before and after forming (b) as well as metallographic cross-section view of the component from [14] (c).

Summary

The scope of this work was the development of a methodology for the numerical inverse calibration of a damage model to describe the failure of a joining zone in hybrid pre-joined semi-finished products made of 100Cr6 and EN AW-6082. For this purpose, local tensile tests were performed at room temperature with miniature tensile samples taken from hybrid semi-finished products. To account for the effect of process relevant forming temperatures, the tests were also carried out at elevated temperatures. The test temperatures were defined based on numerical simulations of the inhomogeneous induction heating and the impact extrusion process. The results showed a strong influence of the sample extraction area and temperature on the achievable bond strength. The damage parameter $t_{t,max}$ was determined inversely by a numerical simulation of the performed tensile tests. The numerically calculated force-displacement curves showed good agreement with the experimental results.

An initial numerical simulation of the impact extrusion process shows that damage occurs in the joining zone. In further investigations, the other parameters of the model are calibrated by supplementary tensile tests with varying the angle between the loading direction and the joining zone of EN AW-6082 as well as 100Cr6 to improve the model quality. Finally, the model will be validated by means of experimental extrusion tests regarding the failure behaviour of the joining zone. The validated model will then be used to evaluate and design concepts such as a counterpressure concept in order to ensure damage-free production of hybrid components.

Acknowledgements

The results presented in this paper were obtained within the Collaborative Research Centre 1153 “Process chain to produce hybrid high-performance components by Tailored Forming” in the subproject C01. The authors would like to thank the German Research Foundation (Deutsche

Forschungsgemeinschaft, DFG, 252662854) for the financial and organisational support of this project. The authors would like to thank the subproject B03 for friction welding of hybrid semi-finished parts and the subproject C04 for support regarding the damage model.

References

- [1] P. Wu, B. Wang, J. Lin, B. Zuo, Z. Li, J. Zhou, Investigation on metal flow and forming load of bi-metal gear hot forging process, *Int. J. Adv. Manuf. Technol.* 88 (2017) 2835-2847. <https://doi.org/10.1007/s00170-016-8973-x>
- [2] R. Leiber, Hybridschmieden bringt den Leichtbau voran, *Aluminium Praxis* (2011) 7-8.
- [3] P. Groche, S. Wohletz, A. Erbe, A. Altin, Effect of the primary heat treatment on the bond formation in cold welding of aluminum and steel by cold forging, *J. Mat. Process. Technol.* 214 (2014) 2040-2048. <https://doi.org/10.1016/j.jmatprotec.2013.12.021>
- [4] B.-A. Behrens, J. Uhe, Introduction to tailored forming, *Prod. Eng. Res. Devel.* 15 (2021) 133-136. <https://doi.org/10.1007/s11740-021-01022-w>
- [5] B.-A. Behrens, D. Duran, D., J. Uhe, T. Matthias, Numerical investigations on the influence of the weld surface and die geometry on the resulting tensile stresses in the joining zone during an extrusion process, 24th Int Conf Mat Form, Liège, Belgique (2021). <https://doi.org/10.25518/esaform21.919>
- [6] F. Töller, S. Löhnert, P. Wriggers, Membrane mode enhanced cohesive zone element, *Eng. Comp.* 39 (2022) 722-743. <https://doi.org/10.1108/EC-08-2020-0489>
- [7] B.-A. Behrens, H. Wester, S. Schäfer, C. Büdenbender, Modelling of an induction heating process and resulting material distribution of a hybrid semi-finished product after impact extrusion, 24th Int Conf Mat Form, Liège, Belgique (2021). <https://doi.org/10.25518/esaform21.574>
- [8] R. Goldstein, B.-A. Behrens, D. Duran, Role of Thermal Processing in Tailored Forming Technology for Manufacturing Multi-Material Components, *Heat Treat Conference* (2017).
- [9] S. Herbst, H. Aengeneyndt, M.J. Maier, F. Nürnberger, Microstructure and Mechanical Properties of Friction Welded Steel-Aluminum Hybrid Components after T6 Heat Treatment, *Mater. Sci. Eng: A* 696 (2017) 33-41. <https://doi.org/10.1016/j.msea.2017.04.052>
- [10] B. Nacke, Ein Verfahren zur numerischen Simulation induktiver Erwärmungsprozesse und dessen technische Anwendung. Dissertation, Hannover (1987).
- [11] G. Lélias, E. Paroissien, F. Lachaud, J. Morlier, Experimental characterization of cohesive zone models for thin adhesive layers loaded in mode I, mode II, and mixed-mode I/II by the use of a direct method, *Int. J. Solid. Struct.* 158 (2019) 90-115. <https://doi.org/10.1016/j.ijsolstr.2018.09.005>
- [12] J. Besson, Continuum Models of Ductile Fracture: A Review, *Int. J. Dam. Mech.* 19 (2010) 3-52. <https://doi.org/10.1177/1056789509103482>
- [13] S. D. Meshram, T. Mohandas, G. M. Reddy, Friction welding of dissimilar pure metals, *J Mat Proc Tech* 184 (2007) 330-337. <https://doi.org/10.1016/j.jmatprotec.2006.11.123>
- [14] B.-A. Behrens, J. Uhe, F. Süer, D. Duran, T. Matthias, I. Ross, Fabrication of steel-aluminium parts by impact extrusion, *Mater. Today: Proceedings* 59 (2022) 220-226. <https://doi.org/10.1016/j.matpr.2021.11.093>